

Reconfigurable Innervation of Modular Soft Machines via Soft, Sticky, and Instant Electronic Adhesive Interlocking

Jaeyoung Yoon, Junghwan Byun, Minjo Park, Hayun Kim, Woongbae Kim, Jinsu Yoon, Kyu-Jin Cho,* and Yongtaek Hong*

Adaptive and extreme changes in shape and configuration are the functional and morphological uniqueness of soft robots, but existing design approaches still rely on the predefined coordination of their “muscle” and “nerve” functions to produce such behaviors. Herein, a strategy is introduced for building modular soft machines that can be innervated in ways that conform to their body extension or shape changes, based on modular soft electronics. The development of soft electronic adhesive interlocking (SEAL) technology allows for instant, robust, and repeatable integration of soft electronic modules that can “innervate” and activate modular soft actuators and machines in a reconfigurable manner. Demonstrations of soft robotic tentacles and their grasping capability show that the robot function can be adapted to or reconfigured within the body with a length extended more than 10 times. The modular strategy presented herein can offer a unique promise to build up future robots with dynamic, reconfigurable functions.

1. Introduction

Recent emergence of robots made of soft materials and structural compliance has underpinned the superiority of nature’s design principle.^[1,2] Beginning with the mimicry of basic biological shape-morphing mechanisms, exemplified by an octopus’ arm^[3,4] or fish’s fin,^[5,6] this newer class of design paradigm has reached the point of harnessing their muscular structures,^[7] material compositions,^[8,9] and embodied locomotion principles.^[10–14] In a similar context, the structure of soft actuators is accordingly based to some extent on the anatomical structure of biological muscle tissues, where muscle cells are innervated and activated by closely coupled somatic motor neurons via the neuromuscular junction.

For example, soft artificial “muscles” are built upon the seamless entanglement with embodied fluid flows (“fluidic nerve”; e.g., pneumatic network^[15–18]) or electronics-induced stimulation (“electronic nerve”; e.g., dielectric elastomer actuator [DEA],^[19,20] Joule-heating-assisted phase transition,^[13,21] and biohybrid stimulation^[9,22,23]) (Figure S1, Supporting Information). In light of this design perspective, existing soft robot systems mostly rely on the predefined coordination of muscles and nerves.


Adaptive and extreme changes in shape and configuration are the functional and morphological uniqueness of soft robots that traditional robots have found difficult to achieve. In fact, studies of robot functions accompanied by large deformation corresponding to several times the initial length, such as soft origami designs^[24–27] or vine-like growing robots,^[28] have highlighted the cutting-edge branch of the soft robot field. Nevertheless, shape-morphing behaviors based on the predefined and limited coordination between “muscles” and “nerves” identify intrinsic hurdles for versatile uses. For example, the actuation profiles of the soft pneumatic origami robots, whose crease patterns are closely coupled with embedded fluidic “nerve” networks, produce only preprogrammed folding/unfolding motions.^[25–27] In this respect, achieving versatile shape-morphing profiles may require dynamic reconfiguration (i.e., selective and reversible attachment or detachment) of both muscle and nerve parts within the robot body. Modular designs as a potential alternative hold promise for an extensive range of structural reconfiguration for both muscle and nerve parts,

J. Yoon, H. Kim, J. Yoon, Y. Hong
Department of Electrical and Computer Engineering
Inter University Semiconductor Research Center (ISRC)
Seoul National University
Seoul 08826, Republic of Korea
E-mail: yongtaek@snu.ac.kr

J. Byun
Physical Intelligence Department
Max Planck Institute for Intelligent Systems
70569 Stuttgart, Germany

M. Park, K.-J. Cho
Department of Mechanical and Aerospace Engineering
Institute of Advanced Machines and Design (IAMD)
Soft Robotics Research Center (SRRC)
Seoul National University
Seoul 08826, Republic of Korea
E-mail: kjcho@snu.ac.kr

W. Kim
Artificial Intelligence and Robotics Institute
Korea Institute of Science and Technology (KIST)
Seoul 02792, Republic of Korea

 The ORCID identification number(s) for the author(s) of this article can be found under <https://doi.org/10.1002/aisy.202300013>.

© 2023 The Authors. Advanced Intelligent Systems published by Wiley-VCH GmbH. This is an open access article under the terms of the Creative Commons Attribution License, which permits use, distribution and reproduction in any medium, provided the original work is properly cited.

DOI: 10.1002/aisy.202300013

thus maximizing the design diversity and functional versatility of soft robots.^[29] For instance, a pneumatically driven modular soft robot, which accounts for the vast majority of the modular design, enables the simultaneous reconfiguration of its body (“muscle”) and fluidic channels (“nerve”) and consequently produces various shape morphing, function, and locomotion that were unattainable by a predefined manner.^[30–36] In addition to the fluidic nerve, the integration of electronic nerves onto DEAs,^[19,20] shape memory alloys,^[37] shape memory polymers,^[38] and phase-transition-based muscles^[13,21] has also been proposed as promising options for modularized soft actuators.

Soft electronics has aided in the design and functional advancement of soft robotics over the past few years.^[39,40] The stretchy feature of the soft electronic system can ideally offer the capabilities of sensing, signal processing, muscle innervation, and control to soft robots with compact and stable connections.^[41] Such benefits bring a clear comparative advantage in many aspects over other existing “nerve” components, such as autonomous fluidic logic circuitry.^[42–45] Given the physical layout and reconfigurable features of modular soft robots, therefore, the modular assembly of soft electronic functions could offer an innovative strategy for functionalizing the robot. Ongoing efforts in this direction include rapid but irreversible siloxane bonding of system level, tailorable electronic modules,^[46] and self-healable reconfiguration of liquid metal interconnects.^[47] Despite such achievements, the irreversible bonding technique and self-healing time (> a few minutes) cause the repeatability and speed issues of innervation for soft robot applications, respectively. Still, none of the existing soft electronic technologies can meet the design or performance requirement of modular soft electronic nerves for reconfigurable modular soft robots.

Here, we introduce a novel strategy for reconfiguring modular soft machines innervated by modular soft electronics, which enrich their workspace and functionalities through both body extension and adaptive innervation (**Figure 1a**). The technical basis for this approach lies in a rapid, robust, and reversible reconfiguration of soft electronic nerves that can be intimately coupled with modular soft actuators and innervate them in a versatile fashion. To achieve these capabilities, we developed a soft, sticky electronic adhesive that combines mechanically interlocking structures with vertically conductive, chemically modified elastomer composites: we call it as “Soft Electronic Adhesive interLocking (SEAL).” The SEAL allows for 1) instant assembly of soft electronic modules that carry more than 10^5 times increase in conductivity between each module within 50 ms once interlocked; 2) robustness of the assembled modules under various mechanical deformations such as pressing, bending, twisting, and stretching; and 3) repeatable and reconfigurable integration of the modules into modular soft actuators and machines for innervation. In combination with adequate designs of electronics and robot modules, the SEAL delivers reconfiguring and shape-changing instructions for the fixed or extended modular soft robot bodies with a length of about 10 times its initial length. The reconfigurable innervation approach presented here would pave a way for next-generation electrically driven soft machines.

2. Results

2.1. Design and Mechanism of SEAL

Our SEAL technology is built from two key components: a soft, sticky, and vertically conductive elastomer composite and a tailorable, soft silver nanowire (AgNW) interconnect (**Figure 1b**). The sticky elastomer composite was made up of chemically modified poly (dimethyl siloxane) (PDMS) matrix within which highly conductive silver-coated nickel microparticles (Ag–Ni, diameter $\approx 10 \mu\text{m}$) were magnetically self-assembled into the form of micropillar arrays (**Figure 1c,d**, and **S2** and **S3**, Supporting Information, for fabrication details). The addition of ethoxylated polyethyleneimine (PEIE) transformed the cross-linking network of PDMS from homogeneous to heterogeneous one, which allowed for a 12-fold increase in the van der Waals force of the surface while maintaining the solid phase.^[48] We additionally defined microscale-corrugated structures at their top surface so as to form compact mechanical interlocking with the AgNW interconnect that greatly complements the adhesive property. The conductive inclusions were successfully aligned within 3 min under a patterned magnetic field of 100 mT even inside the sticky polymer matrix with a relatively high viscosity, and made the entire composite vertically conductive (out-of-plane direction).^[49,50] In addition to the morphological and electrical characteristics, importantly, this sticky elastomer composite could be formed directly onto the soft electronic module such that it could play a perfect role as an electronic adhesive between various functional modules. For the tailorable soft interconnect, a corrugated microstructure of AgNW networks was introduced, and its performance was optimized to have a high electrical conductivity of 800 S m^{-1} and reliable stretchability up to 50% without any significant conductivity drop (**Figure S4**, Supporting Information).^[46] The tensile test result performed on SEAL revealed Young’s modulus of 0.34 MPa, which is notably lower than that of PDMS (10:1). Specifically, the modulus of SEAL was found to be approximately one tenth that of PDMS as shown in **Figure S5f**, Supporting Information.

The complementary nature arising from the tripartite coupling between strong van der Waals adhesion, mechanical interlocking, and high conductivity underlies the mechanism of SEAL (**Figure 1e**). Although the sticky composite itself has very weak in-plane conduction paths (**Figure 1e**, left; and **Figure S3**, Supporting Information), the strong and robust interlocking with AgNW interconnects enables superb conduction paths through every electronic module (**Figure 1e**, right), possibly resulting in programmable electronic innervation when coupled with soft actuators. The innervation process through the SEAL, which was done by manual assembly with gentle pressure, achieved over five orders of magnitude decrease in resistance with repeatable and reliable properties (**Figure 1f**); and its response was rapid (<50 ms) (**Figure 1g**) and robust (**Figure 1h**) enough to facilitate practical modular assembly in situ (**Figure 1i**).

2.2. Electrical and Adhesive Characterization of SEAL

To further investigate the principal characteristics and performance of the SEAL, we prepared a set of samples ($1 \times 5 \text{ cm}^2$) with different degrees of morphology, conductivity, and

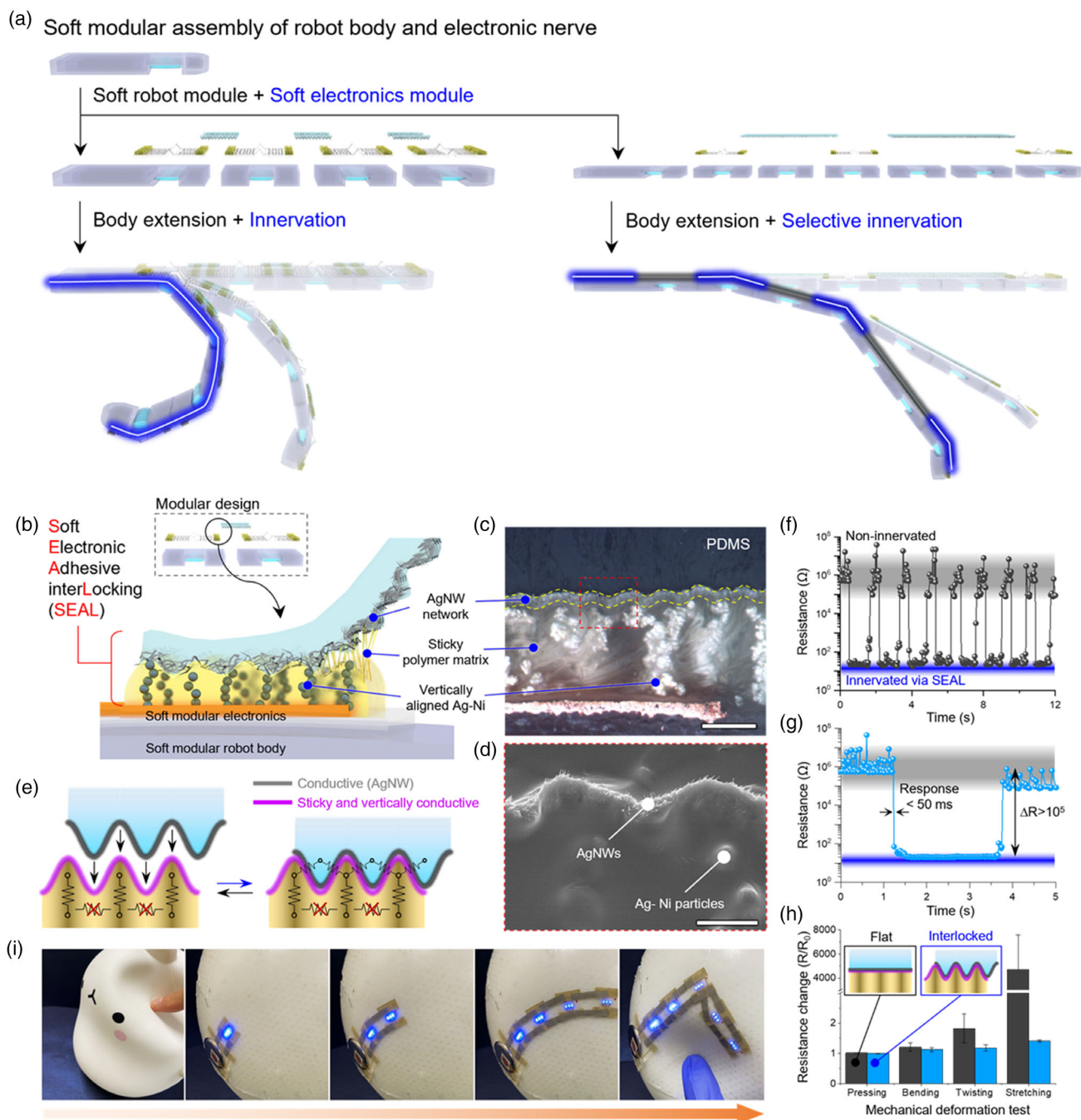


Figure 1. Design concept of soft electronic adhesive interlocking (SEAL) for reconfigurable innervation of modular soft machines. a) Modular assembly of soft robot body and electronic nerves enables both body extension and its reconfigurable innervation. b) Design concept of SEAL based on the tripartite coupling between enhanced van der Waals adhesion, mechanical interlocking, and high electrical conductivity. See Figure S2, Supporting Information, for the detailed fabrication steps. Scanning electron microscopy (SEM) images of c) the SEAL and d) its magnified view. Scale bars, 30 μm in (c) and 10 μm in (d). e) Mechanism of SEAL. f) Cyclic responses of the SEAL-mediated electronic innervation demonstrating repeatable and reliable assembly between soft electronic modules. g) Typical response of the SEAL-mediated innervation showing the response time of < 50 ms for each assembly process and drastic increase in electrical conductivity by more than five orders of magnitude. h) Mechanical robustness of the SEAL-mediated innervation in comparison with the same adhesive without mechanically interlocking structures. i) Modular assembly demonstration of soft light-emitting modules in situ.

stickiness, and performed 180° peeling tests using a universal testing machine (Instron-5543, Instron Inc.) (Figure S5a, Supporting Information). The results first show that the SEAL

without any interlocking structure produced the adhesion force of only 0.01 N cm^{-1} , whereas the presence of corrugated structures improved it by more than five times (Figure 2a).

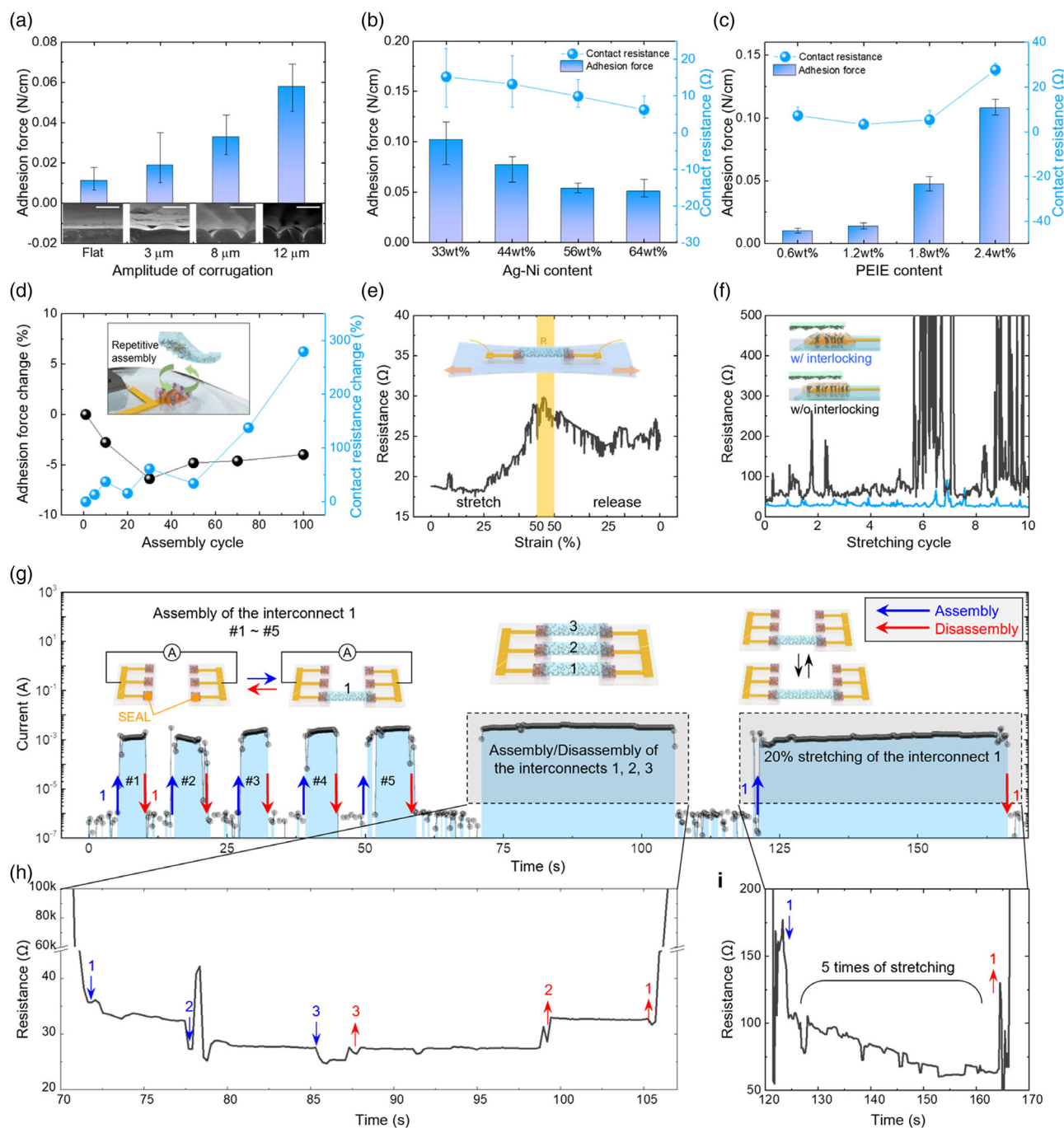


Figure 2. Electrical and adhesive characterization of SEAL. a) Effect of mechanical interlocking on adhesive properties. Inset SEM images show the typical corrugated microstructures with different amplitudes. Scale bars, 20 μm . Electrical and adhesive properties as a function of b) Ag–Ni microparticles, c) polyethyleneimine (PEIE) contents, and d) assembly cycle. Mechanical robustness and stretchy tolerance of the assembled electronic modules e) under 50% strain and f) cyclic stretching of 30% strain in comparison with the sample without mechanical interlocking. g,h) Continuous, real-time responses of the SEAL-mediated soft modular electronic system with dynamic and reconfigurable assembly/disassembly processes and i) during 20% stretching of 5 cycles.

This phenomenon arises from the change in contact area as the amplitude of corrugation increases, advocating our design approach that mechanical interlocking structures work complementarily with van der Waals adhesion. The conductivity of the

SEAL relies not only on the volume (or weight) ratio of Ag–Ni microparticles against that of polymer matrix, but also on their vertical alignment induced by a patterned magnetic field;^[49,50] therefore, a trade-off necessarily occurs between the conductivity

and stickiness (adhesion force) (Figure 2b,c). For example, as the amount of Ag–Ni microparticles within the mixture increased up to 64 wt%, the sticky composite gained conductivity while it gradually lost its adhesion (Figure 2b). Similarly, as we increased the content of PEIE, which is a chemical agent that makes PDMS sticker,^[48] the adhesion force drastically increased to more than 0.1 N cm⁻¹, but the conductivity could not be matched to the ideal value for use (Figure 2c). As a consequence, we balanced these contents by taking the values of 56 wt% of Ag–Ni microparticles and 1.8 wt% of PEIE, and obtained the optimal performance of the SEAL which has a contact resistance of $\approx 10 \Omega$ and an adhesion force of $\approx 0.05 \text{ N cm}^{-1}$.

The robustness, reliability, and potentiality for practical modular assembly were explored by a set of experimental cyclic tests in terms of adhesion and mechanical stretching. First, we observed that the effect of repeated assembly and disassembly on both electrical and adhesive performance was negligible up to 50 times; however, in subsequent cycles, the contact resistance significantly increased and reached about three times the initial value whereas the adhesive characteristics remained nearly unchanged up to 100 times, although the adhesive characteristics degrade by about 30% after 10 000 repetitions of assembly (Figures 2d and S5e, Supporting Information). This behavior of degradation stems from the fatigue-induced fracture of AgNWs embedded in the surface of AgNW interconnects upon repetitive assembly/disassembly processes during which the fractured AgNWs remain as residues on the SEAL pad (Figure S6a, Supporting Information). Although this modular connection reached its yield around 50 times of repetitive assembly, we could solve this issue by introducing a fresh interconnect which restored the contact resistance to its initial level (Figure S6b,c, Supporting Information). In addition to the tolerance to repetitive adhesion, it is necessary to obtain a sufficient level of stretchability that allows the modular system to stably innervate and control soft machines under their continuum deformation. We found that the electrical characteristics of the SEAL and interconnect system could be maintained up to the external strain of 50% without the contact failure at the SEAL interface (Figure 2e). This stretchy–tolerance attributes mainly to the existence of the corrugated mechanical interlocking structure (Figures 1i and 2f). Due to the 1D pattern, the performance of SEAL has an angle dependency, which varies about 30% depending on the angle of alignment (Figure S5b,c, Supporting Information). The optimized electronic modules could work without contact failure under over 5,000 cycles of 25% stretching (Figure S5d, Supporting Information).

Based on these characterizations, we explored in situ, real-time responses of consecutive reconfiguration of the SEAL-based soft modular electronic system (Figure 2g–i). We prepared three individual interconnects (1, 2, 3) and two soft electronic modules, each of which has three SEAL pads for connection (see the inset schematics in Figure 2g). Long-term, dynamic, and reconfigurable assembly processes were conducted based on three distinctive regimes: 1) repetitive assembly/disassembly of the interconnect 1, 2) sequential assembly of the interconnects 1–3 in order and their disassembly, and 3) assembly and cyclic stretching (20% strain) of the interconnect 1. The results show that the instantaneous formation (<50 ms; see Figure 1h) of

electrical conduction paths via SEALs enabled rapid, robust, and repeatable reconfiguration of soft electronic modules in situ.

2.3. Design and Characterization of Modular Soft Robots Innervated by Modular Electronic Nerves

The optimized SEAL technology and the resultant soft modular electronics can form the basis of entirely reconfigurable soft machines in which the site of innervation and activation can be controlled by the selective formation of “electronic nerves” instead of the predefined design. As an artificial epidermis that can diversify the innervation paths, this electronic nerve could be closely coupled with the robot and actuate it. Figure 3a shows the exploded-view schematic illustration of the soft robot built upon the modular architectures of both soft electronic nerve parts and soft muscle parts. Each robot module consists of a 3D printed body, a muscle, and a joint that can be mechanically interlocked with other modules. The robot module is innervated by the soft modular electronic nerve based on the seamless bonding via an adhesive layer made of the same base materials (PEIE/PDMS) as the SEAL (see Figure S7, Supporting Information, for fabrication process). The actuation mechanism of the muscle is similar to that of a pouch motor,^[51] where the muscle containing low-boiling-point fluorinated solvents (1-methoxyheptafluoropropane [C₃F₇OCH₃]) with a boiling point of 34 °C) undergoes huge changes in volume through a heat-driven liquid-to-gas phase transition when locally heated up by a soft electronic heater module ($\approx 40 \text{ }^\circ\text{C}$),^[13,21] and this volume increase produces a bending motion while being geometrically constrained by its own deformation (Figure 3b). Figure 3c shows a typical transient response of the single-module soft actuator integrated with the modular soft electronic nerve. Upon the current input of 80 mA, the maximum temperature generated by the heater reached $\approx 70 \text{ }^\circ\text{C}$ within 35 s, which produced an effective bending motion of the actuator up to $\approx 30^\circ$. We also observed that during the first $\approx 15 \text{ s}$ of heating, a geometric buckling process that caused a backward motion occurred in the muscle. This is because when the muscle was assembled onto the robot body by an epoxy glue and adhesive spray, a prestrain was inherently applied to the soft robot joint which changed the equilibrium point of the joint in the low-pressure regime.

Attractive features of the proposed modular soft robot design include a compact assembly between every robot part (i.e., body, muscle, and nerve) as well as a great deal of design freedom for versatile robot function. To showcase the potential benefits, we prepared a bunch of robot modules (Figure 3d) and electronic nerve modules (Figure 3e) and demonstrated an in situ, compact assembly of a fully integrated soft modular robotic finger consisting of three modules (Figure 3f; see Figure S8, and Video S1, Supporting Information, for the assembly process). This approach allowed us to achieve not only the physical body extension of the robot system by several times its initial length but also the adaptive innervation process so that the muscle function can be adapted to or maintained within the extended body form factor (Figure 3g, top; Video S2, Supporting Information). To be specific, if a robot consists of only one single joint (module 1), it is enough to assemble one electronic nerve (heater) to actuate it; however, if the robot is extended to have two (module

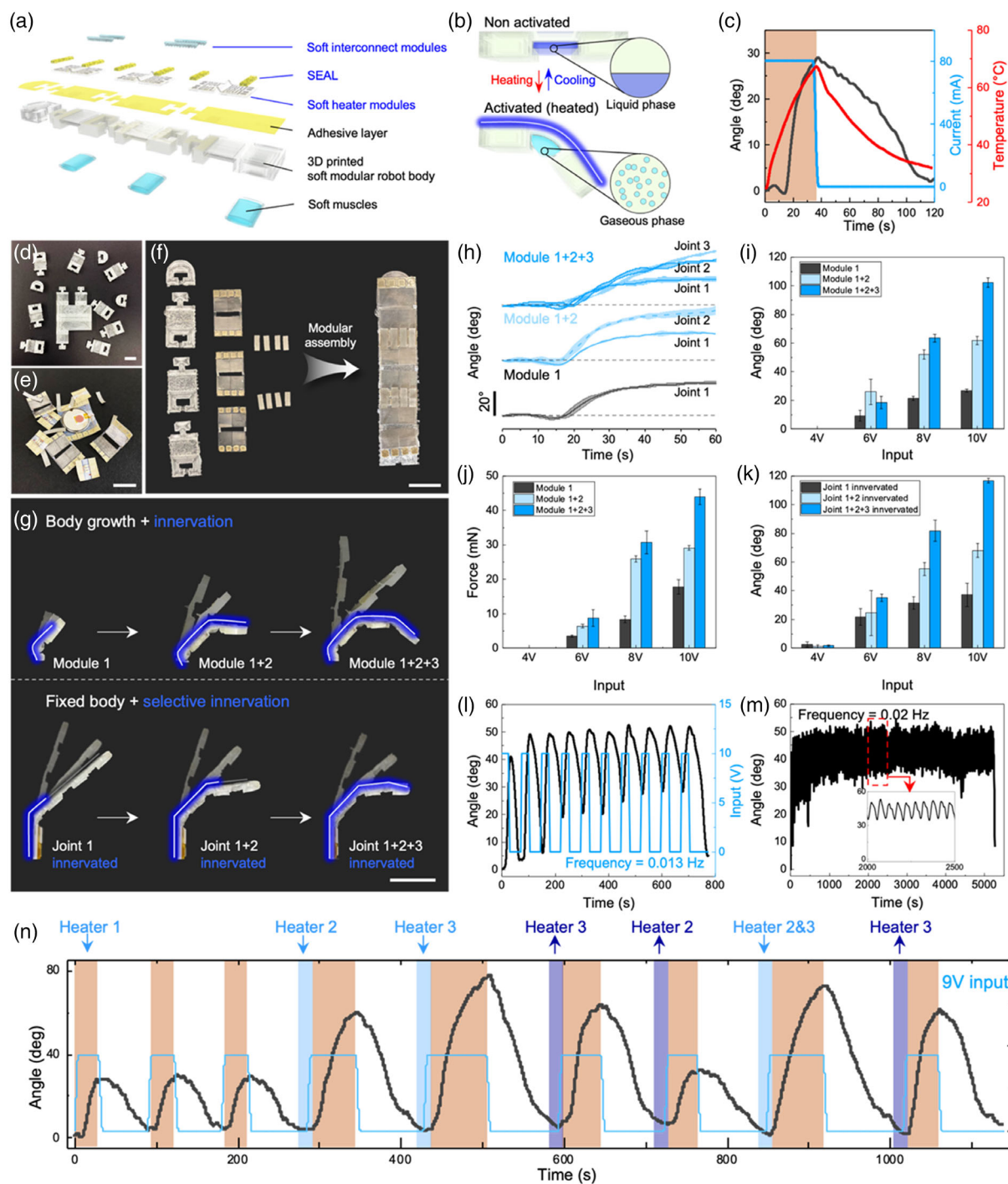


Figure 3. Design and characterization of modular soft robots innervated by modular electronic nerves. a) Exploded-view schematic illustration of a modular soft robot consisting of soft muscles, 3D printed robot modules, electronics modules, and SEAL. See Figure S7, Supporting Information, for the detailed fabrication steps. b) Actuation mechanism of the unit soft robot module consisting of the liquid-filled muscle and 3D printed robot body. c) Typical actuation profile (angle) of the unit robot module in response to heating of 40 s. Photographs of d) 3D printed robot modules, e) electronic modules with SEAL, and f) their assembly. All scale bars, 2 cm. g) Actuation sequences of extending 3-module soft robots innervated by modular soft electronic nerves. Scale bar, 5 cm. Actuation performance of the extending modular robots: transient responses of each joint for each extension sequence, from module 1 to module 1 + 2 + 3 as depicted in Figure 2 g, h) top, i) saturated responses, and j) fingertip forces as a function of the input voltage. k) Actuation performance of the 3-module robot with selective innervation as a function of the input voltage. Robot actuation l) with a repetition frequency of 0.017 Hz and m) repeatability of a soft robot under 10 V input. n) Continuous, real-time responses of the 3-module soft robot with dynamic and reconfigurable innervation by assembly/disassembly of electronic modules.

1 + 2) or three joints (module 1 + 2 + 3), additional nerves should be formed to meet the full potential of its extended body. In addition to this basic design scheme, the capability of full reconfiguration in the body and nerve part also suggested nontrivial, versatile responses of the robotic finger by selective innervation without any electrical programming (Figure 3g, bottom; Video S3, Supporting Information).

We quantitatively investigated the output performance of the modular robot actuation to obtain the accessible range of work-space and force for potential applications. Herein, the bending angle and the fingertip force were two main parameters, each of which was measured respectively by the experimental setup as shown in Figure S9, Supporting Information. First, we measured the transient response of every joint for the designs with module 1, module 1 + 2, and module 1 + 2 + 3 (see Figure 3g, top), when activated by the electronic nerve with the input of 10 V (corresponding to 67, 110, 147 mA, respectively). The results suggested that each joint clearly followed the typical response profile even including the initial (0–15 s) buckling process as shown in Figure 3c (Figure 3h). We also found that the effect of input power and the number of activated joints predominantly contributed to the output bending motion (up to $\approx 110^\circ$) (Figure 3i) and force (up to ≈ 45 mN) (Figure 3j) in a nearly linear fashion. This behavior originates from the fact that the more heat generated, the greater the volume change, which in turn, leads to an increase in the bending stiffness of the robot. Similar results observed in the output performance of the 3-module soft robotic finger with selective innervation suggested that the innervation path, controlled by the modular assembly strategy, could determine the robot function, in addition to the design of the robot body (Figure 3k). The actuation of modular robots can be achieved at a range of frequencies through modulation of the duty cycle of the input voltage (Figure 3l and S11, Supporting Information). Furthermore, Figure 3m demonstrates that the modular soft robot assembled with an electronic nerve can repeat actuation even at repetitions of more than 100 times with no significant degradation.

We finally carried out the long-term and dynamic reconfiguration of the modular soft robot to verify the instantaneous innervation and the corresponding responses of the robot (Figure 3n). The 3-module robotic finger was used in the test with the constant input of 9 V. On top of the results shown in Figure 2g, it was revealed that the SEAL-induced conduction paths and electronic nerve networks, formed instantly onto the robot body by modular soft electronics, successfully provided the sequence of spatially coordinated “activation cues” (heat in this case) at the site of interest and the resulting robot actuation consequently demonstrated the effectiveness of reconfigurable innervation of soft machines.

2.4. Reconfigurable Innervation of Modular Soft Robots

Key benefits of our approach arise from the capabilities of body extension to the desired length and of reconfigurable innervation adaptive to the elongated body. To show an extreme case of prototypical examples, we demonstrated a class of robotic tentacles that can extend, but are not limited, to 10 times their initial length and get innervated throughout their extended bodies

in a programmable manner without electrical programming (Figure 4a). The robotic tentacle grew up by the sequential assemblies of constituent robot unit modules, and became functionalized by soft modular electronic nerves. Upon activation, its pattern of movement could range from fingertip movement to, if necessary, large deformations throughout the entire body depending on the site of innervation, providing potential capabilities of shape morphing suitable for target objects, functions, and environments (Figure 4a; Video S4, Supporting Information).

The modular design of soft robots and their capabilities of reconfigurable innervation by modular soft electronics may provide ideal platforms for the tasks that robots with predefined layouts and functions cannot address. As an illustrative example, we demonstrated a set of soft robotic grippers consisting of three robotic tentacles (Figure 4b–e). First, the positioning of the robotic tentacles in the form of human hands allowed the gripper to produce movements with small curvatures when fully innervated (Figure 4b). Notably, the total power consumption of the gripper was at an appropriate level (≈ 5.4 W; 1.8 W [= 12 V \times 150 mA] per each robotic tentacle) that could be driven using commercially available batteries. This implies that the robots or machines built upon our design strategy can be highly compact and untethered with minimal computing units and appendages, showing benefits over existing pneumatically driven modular robot designs (Figure 4c).^[29–36] To further validate the effectiveness of our concept, we developed a gripper that can extend from 4 to 25 cm in length with selective innervation (Figure 4d; Video S5, Supporting Information, for simulation of robotic tentacles). In particular, the sites of innervation were limited to three robot modules located at the fingertip part to achieve both reconfigurable innervation and effective grasping. This gripper successfully demonstrated universal gripping of various, lightweight objects (Figure 4e; Video S6, Supporting Information). The maximum weight that our gripper can grip is estimated using a coefficient of static friction (3.54) of the fingertip to be about 49 g based on three fingers. Still, it may vary depending on the number of fingers or the shape and surface of the object (Figure S10, Supporting Information).

3. Discussion

In this work, we have described advances in robotic reconfigurability that point the way toward new methods of designing electrically innervated soft machines. We have proposed and validated an entirely modular design achieving a high degree of both body extension and adaptive innervation of soft machines for versatile shape morphing and robot applications. Combined aspects of micro-corrugated mechanical interlocking, enhanced van der Waals adhesion, and magnetically aligned vertical electrical conduction (named, “SEAL”) allowed for rapid, robust, and repeatable assembly of soft electronic modules in a manner that formed reconfigurable electronic nerves of soft machines. The soft robot presented here was a prototypical design that could be easily 3D printed, modularized, and integrated seamlessly with soft electronics. The results showed that the robot could extend its body and be innervated and actuated either entirely or site-selectively by electronic nerve distribution, providing

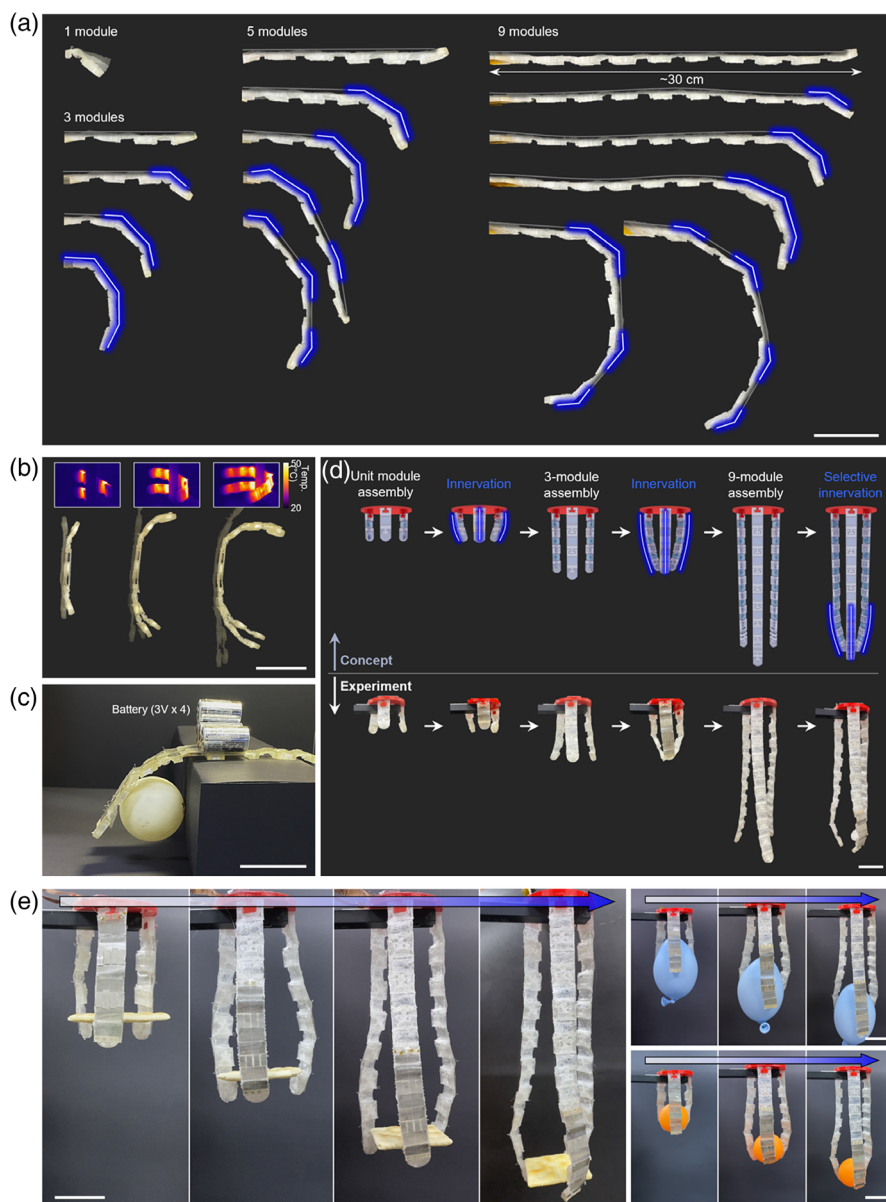


Figure 4. Reconfigurable innervation of modular soft machines. a) Multi-module soft robotic tentacles showing extreme shape changes by both body extension and reconfigurable innervation, b) a soft robotic gripper consisting of 3-module robotic tentacles and its actuation heat map (inset). c) Untethered design of the gripper shown in (b). d,e) Concept and demonstration of a soft robotic gripper consisting of 9-module robotic tentacles that can extend and be selectively innervated for grasping capabilities. All scale bars, 5 cm.

potential capabilities to suit targeted applications. Although the robot applications we presented here were limited to the soft robotic grippers, it is believed that our approach could readily broaden its potential applications by diversifying the design of the unit robot module and the way of its assemblies.

We focused, in the current robot design, on the validation of dynamic modular assembly with extreme shape changes such as body extension and shape morphing; hence, there still remains much room for improvement in actuation time and force, currently limited to ≈ 40 s and ≈ 50 mN, respectively. Optimizing the volume of liquid encased within the muscle and increasing

the heat conductivity of the robot body would be a possible engineering solution. Further, the use of high-performance DEAs^[19,20] or electrically driven artificial muscles^[52,53] and pumps^[54,55] might provide a more practical set of robot applications. The employment of active, autonomous assembly technologies (e.g., magnets) will further augment the autonomy and functionality of reconfigurable modular robots. Focusing on the SEAL, enhancing the length of AgNW interconnects for soft electronic nerves is necessary. This can lead to the development of larger robots, thereby expanding the workspace of soft modular robots. However, achieving this may require new fabrication

methods for interconnects. Given all these features, we expect that our approach would make a step toward a new generation of reconfigurable and environment-adaptive robots.

Supporting Information

Supporting Information is available from the Wiley Online Library or from the author.

Acknowledgements

J.Y. and J.B. contributed equally to this work. This work was supported in part by the Display Center of Samsung Display and Seoul National University and in part by the National Research Foundation of Korea (NRF) grant funded by the Korean Government (MSIT) (Grant no. NRF-2016R1A5A1938472). J.B. thanks the Alexander von Humboldt Foundation for financial support.

Conflict of Interest

The authors declare no conflict of interest.

Data Availability Statement

The data that support the findings of this study are available from the corresponding author upon reasonable request.

Keywords

adhesive interlocking, modular soft electronics, modular soft robot, reconfigurable robot, soft modular assembly

Received: January 17, 2023

Revised: March 23, 2023

Published online:

- [1] D. Rus, M. T. Tolley, *Nature* **2015**, 521, 467.
 [2] S. Kim, C. Laschi, B. Trimmer, *Trends Biotechnol.* **2013**, 31, 287.
 [3] C. Laschi, M. Cianchetti, B. Mazzolai, L. Margheri, M. Follador, P. Dario, *Adv. Rob.* **2012**, 26, 709.
 [4] M. Cianchetti, M. Calisti, L. Margheri, M. Kuba, C. Laschi, *Bioinspiration Biomimetics* **2015**, 10, 035003.
 [5] T. Li, G. Li, Y. Liang, T. Cheng, J. Dai, X. Yang, B. Liu, Z. Zeng, Z. Huang, Y. Luo, T. Xie, W. Yang, *Sci. Adv.* **2017**, 3, e1602045.
 [6] A. D. Marchese, C. D. Onal, D. Rus, *Soft Rob.* **2014**, 1, 75.
 [7] A. Ramezani, S.-J. Chung, S. Hutchinson, *Sci. Rob.* **2017**, 2, eaal2505.
 [8] J. C. Nawroth, H. Lee, A. W. Feinberg, C. M. Ripplinger, M. L. McCain, A. Grosberg, J. O. Dabiri, K. K. Parker, *Nat. Biotechnol.* **2012**, 30, 792.
 [9] S.-J. Park, M. Gazzola, K. S. Park, S. Park, V. Di Santo, E. L. Blevins, J. U. Lind, P. H. Campbell, S. Dauth, A. K. Capulli, F. S. Pasqualini, S. Ahn, A. Cho, H. Yuan, B. M. Maoz, R. Vijaykumar, J.-W. Choi, K. Deisseroth, G. V. Lauder, L. Mahadevan, K. K. Parker, *Science* **2016**, 353, 158.
 [10] H.-T. Lin, G. G. Leisk, B. Trimmer, *Bioinspiration Biomimetics* **2011**, 6, 026007.
 [11] Y. Tang, Y. Chi, J. Sun, T.-H. Huang, O. H. Maghsoudi, A. Spence, J. Zhao, H. Su, J. Yin, *Sci. Adv.* **2020**, 6, eaaz6912.
 [12] R. K. Katzschmann, J. Delpreto, R. MacCurdy, D. Rus, *Sci. Rob.* **2018**, 3, eaar3449.

- [13] J. Byun, M. Park, S.-M. Baek, J. Yoon, W. Kim, B. Lee, Y. Hong, K.-J. Cho, *Sci. Rob.* **2011**, 6, eaab0637.
 [14] T. Bujard, F. Giorgio-Serchi, G. D. Weymouth, *Sci. Rob.* **2021**, 6, eabd2971.
 [15] R. F. Shepherd, F. Ilievski, W. Choi, S. A. Morin, A. A. Stokes, A. D. Mazzeo, X. Chen, M. Wang, G. M. Whitesides, *Proc. Natl. Acad. Sci. U.S.A.* **2011**, 108, 20400.
 [16] A. D. Marchese, R. K. Katzschmann, D. Rus, *Soft Rob.* **2015**, 2, 7.
 [17] M. T. Tolley, R. F. Shepherd, B. Mosadegh, K. C. Galloway, M. Wehner, M. Karpelson, R. J. Wood, G. M. Whitesides, *Soft Rob.* **2014**, 1, 213.
 [18] B. Mosadegh, P. Polygerinos, C. Keplinger, S. Wennstedt, R. F. Shepherd, U. Gupta, J. Shim, K. Bertoldi, C. J. Walsh, G. M. Whitesides, *Adv. Funct. Mater.* **2014**, 24, 2163.
 [19] C. Christianson, N. N. Goldberg, D. D. Deheyn, S. Cai, M. T. Tolley, *Sci. Rob.* **2018**, 3, eaat1893.
 [20] J. Shintake, V. Cacucciolo, H. Shea, D. Floreano, *Soft Rob.* **2018**, 5, 466.
 [21] A. Miriyev, K. Stack, H. Lipson, *Nat. Commun.* **2017**, 8, 596.
 [22] Y. Morimoto, H. Onoe, S. Takeuchi, *Sci. Rob.* **2018**, 3, eaat4440.
 [23] C. Cvetkovic, R. Raman, V. Chana, B. J. Williams, M. Tolishe, P. Bajaja, M. S. Sakard, H. H. Asadad, M. T. A. Saif, R. Bashir, *Proc. Natl. Acad. Sci. U.S.A.* **2014**, 111, 10125.
 [24] W. Kim, J. Byun, J.-K. Kim, W.-Y. Choi, K. Jakobsen, J. Jakobsen, D.-Y. Lee, K.-J. Cho, *Sci. Rob.* **2019**, 4, eaay3493.
 [25] S.-J. Kim, D.-Y. Lee, G.-P. Jung, K.-J. Cho, *Sci. Rob.* **2018**, 3, eaar2915.
 [26] R. V. Martinez, C. R. Fish, X. Chen, G. M. Whitesides, *Adv. Funct. Mater.* **2012**, 22, 1376.
 [27] S. Li, D. M. Vogt, D. Rus, R. J. Wood, *Proc. Natl. Acad. Sci. U.S.A.* **2017**, 114, 13132.
 [28] E. W. Hawkes, L. H. Blumenschein, J. D. Greer, A. M. Okamura, *Sci. Rob.* **2017**, 2, eaan3028.
 [29] C. Zhang, P. Zhu, Y. Lin, Z. Jiao, J. Zou, *Adv. Intell. Syst.* **2020**, 2, 1900166.
 [30] J.-Y. Lee, W.-B. Kim, W.-Y. Choi, K.-J. Cho, *IEEE Rob. Autom. Mag.* **2016**, 23, 30.
 [31] E. P. Perez-Guagnelli, presented at *2018 IEEE Conf. Robotics and Automation (ICRA)*, Brisbane, QLD, Australia, May 2018.
 [32] Z. Jiao, C. Ji, J. Zou, H. Yang, M. Pan, *Adv. Mater. Technol.* **2019**, 4, 1800429.
 [33] Z. Jiao, C. Zhang, W. Wang, M. Pan, H. Yang, J. Zou, *Adv. Sci.* **2019**, 6, 1901371.
 [34] J. Zou, Y. Lin, C. Ji, H. Yang, *Soft. Rob.* **2018**, 5, 164.
 [35] M. A. Robertson, O. C. Kara, J. Paik, *Int. J. Rob. Res.* **2021**, 40, 72.
 [36] M. A. Robertson, J. Paik, *Sci. Rob.* **2017**, 2, eaan6357.
 [37] X. Huang, K. Kumar, M. K. Jawed, A. M. Nasab, Z. Ye, W. Shan, C. Majidi, *Adv. Mater. Technol.* **2019**, 4, 1800540.
 [38] B. Jin, H. Song, R. Jiang, J. Song, Q. Zhao, T. Xie, *Sci. Adv.* **2018**, 4, eaao3865.
 [39] F. Hartmann, M. Drack, M. Kaltenbrunner, *Sci. Rob.* **2018**, 3, eaat9091.
 [40] B. Shih, D. Shah, J. Li, T. G. Thuruthel, Y.-L. Park, F. Iida, Z. Bao, R. Kramer-Bottiglio, M. T. Tolley, *Sci. Rob.* **2020**, 5, eaaz9239.
 [41] J. Byun, Y. Lee, J. Yoon, B. Lee, E. Oh, S. Chung, T. Lee, K.-J. Cho, J. Kim, Y. Hong, *Sci. Rob.* **2018**, 3, eaas9020.
 [42] M. Wehner, R. L. Truby, D. J. Fitzgerald, B. Mosadegh, G. M. Whitesides, J. A. Lewis, R. J. Wood, *Nature* **2016**, 536, 451.
 [43] D. J. Preston, P. Rothemund, H. J. Jiang, M. P. Nemitz, J. Rawson, Z. Suo, G. M. Whitesides, *Proc. Natl. Acad. Sci. U.S.A.* **2019**, 116, 7750.
 [44] D. J. Preston, H. J. Jiang, V. Sanchez, P. Rothemund, J. Rawson, M. P. Nemitz, W.-K. Lee, Z. Suo, C. J. Walsh, G. M. Whitesides, *Sci. Rob.* **2019**, 4, eaaw5496.

- [45] J. D. Hubbard, R. Acevedo, K. M. Edwards, A. T. Alsharhan, Z. Wen, J. Landry, K. Wang, S. Schaffer, R. D. Sochol, *Sci. Adv.* **2021**, *7*, eabe5257.
- [46] J. Yoon, Y. Joo, E. Oh, B. Lee, D. Kim, S. Lee, T. Kim, J. Byun, Y. Hong, *Adv. Sci.* **2019**, *6*, 1801682.
- [47] J. Kang, D. Son, O. Vardoulis, J. Mun, N. Matsuhisa, Y. Kim, J. Kim, J. B.-H. Tok, Z. Bao, *Adv. Mater. Technol.* **2019**, *4*, 1800417.
- [48] S. H. Jeong, S. Zhang, K. Hjort, J. Hilborn, Z. Wu, *Adv. Mater.* **2016**, *28*, 5830.
- [49] S. Kim, J. Byun, S. Choi, D. Kim, T. Kim, S. Chung, Y. Hong, *Adv. Mater.* **2014**, *26*, 3094.
- [50] E. Oh, J. Byun, B. Lee, S. Kim, D. Kim, J. Yoon, Y. Hong, *Adv. Electron. Mater.* **2017**, *3*, 1600517.
- [51] R. Niiyama, X. Sun, C. Sung, B. An, D. Rus, S. Kim, *Soft. Rob.* **2015**, *2*, 59.
- [52] E. Acome, S. K. Mitchell, T. G. Morrissey, M. B. Emmett, C. Benjamin, M. King, M. Radakovitz, C. Keplinger, *Science* **2018**, *359*, 61.
- [53] N. Kellaris, V. G. Venkata, G. M. Smith, S. K. Mitchell, C. Keplinger, *Sci. Rob.* **2018**, *3*, eaar3276.
- [54] V. Cacciolo, J. Shintake, Y. Kuwajima, S. Maeda, D. Floreano, H. Shea, *Nature* **2019**, *572*, 516.
- [55] R. S. Diteesawat, T. Helps, M. Taghavi, J. Rossiter, *Sci. Rob.* **2021**, *6*, eabc3721.